Reduction of Energy Consumption by Optimized Robot Cell Design

Eggers, K.; Hansen, C.; Kotlarski, J.; Ortmaier, T.

ABSTRACT

This paper presents an approach to reduce the energy consumption of industrial robots by optimizing the position of the robot base platform. The approach utilizes a comprehensive energy model for electrical drive systems with DC-bus coupling. The position is optimized for a predefined task in terms of energy consumption and the energy saving potential is analyzed. The results are compared to existing approaches that do not consider the DC-bus energy exchange and it is shown that the utilization of a comprehensive model helps in further improving the energy efficiency. The impact of the base position on the energy consumption is examined by varying the position in a discrete grid. The optimization takes kinematic and dynamic boundaries into account.

1 INTRODUCTION

In the industrial sector, the improvement of energy efficiency constantly gains in importance due to various reasons, e.g. rising energy prices, carbon dioxide emission regulations, and marketing purposes. These evolutions intensify the need of methods to increase the energy efficiency of electrically actuated mechatronic systems. In Germany (as an exemplary industrial country), more than 70 % of the industrial electrical energy consumption is caused by electrical drives [1]. An energetically efficient application of industrial robotic systems can be achieved with consideration of the following layout instructions:

- reasonable dimensioning (robot size and workload),
- reduction of moved masses, either by relocation of additional masses or by utilization of lightweight materials [2],
- utilization of high efficient servo drive components (motors, inverters) [3],
- usage of recuperating supply modules [4].

Even so, all of the above mentioned improvements have certain drawbacks. Standardized robots allow only limited freedom of choice, and, thus, restrict the adaption to the application. Lightweight materials need to fulfill the rigidity requirements and have higher acquisition costs. The latter also applies for recuperating supply modules. Further, the

modules might have negative backlash on the energy grid. Lastly, high efficient servo drive components are already state-of-the-art for industrial robots and offer sparse improvement potential. Alternatively, energy efficiency can be enhanced by software optimization. For example, several publications focus on improving the trajectory planning:

- reduction of mechanical and electrical losses by avoidance of unfavorable operating points, e.g. featuring high actuation speeds (viscous friction losses) and high torques (leading to high actuator currents and, therefore, resistive losses) [5],
- reduction of brake resistor energy dissipation by optimization of DC-bus energy exchange [6].

This paper shows that the energy efficiency can be further improved by optimization of the robot cell design, i.e. by proper positioning of the robot base with respect to the desired task space path. The method can be applied parallel to the enhancements described above and requires no hardware acquisitions except a possible concrete socket. In many applications, an industrial robot processes a single task for his whole lifespan, e.g. spot welding a certain part or moving a specific workpiece in automotive production. Nonetheless, in most production lines, the workspace is often used as the only criterion to determine a robot's base position, although research has shown that the variation of the robot base (or the workpiece) position can be utilized to optimize various performance attributes, e.g. the travel time [7] or the manipulability [8].

In [9], the first approach to find the energy-optimal workpiece location in a robot's workspace is presented. However, the considered robot's drives have no DC-bus coupling. Hence, the deriving effects and possible benefits are not regarded. Further, the approach focuses on minimizing the motor losses, not the system's overall energy consumption, which is a big difference especially for DC-bus coupled systems (which is common for state-of-the-art industrial robots). Hence, it is worth to readdress this topic by combining the findings of [9] with a more detailed and complex energy model as presented in [6]. The results of the two modeling and optimization concepts are

compared and it is shown that the detailed model leads to more accurate results as well as additional energy saving potential. It should be noted that the displacement of the robot base directly affects the joint space trajectories, and, consequently, the trajectory time, the amount and distribution of losses, and the DC-bus energy exchange. The energy consumption is calculated for discretely distributed robot base positions for an exemplary spot-welding task. The article is organized as follows. Section 2 explains the simulation environment including the cost function used to determine the energy consumption of a mechatronic system. In Section 3, the optimization problem with its constraints is expounded. Section 4 presents the utilized exemplary task and discusses the simulation results of a discrete variation of the base position. The paper closes with a conclusion and a short outlook on future works in Section 5.

2 MODELING OF A ROBOT'S ENERGY DEMANDS

The axes of industrial serial robots are typically actuated by inverter controlled three-phase synchronous servo motors, as shown in Fig. 1. For mechatronic systems with multiple axes, there is usually only one supply module for all axes of the system. Thus, the comprehensive servo drive system consists of a single supply module, six servo-inverters, and six synchronous motors. Thereby, the DC-buses of the axes are coupled, which enables energy exchange between axes in motor and generator operating phases. In this paper, exemplarily a Cloos QRC350 welding robot, a classical 6-DOF serial industrial robot, is considered. The kinematic configuration of the robot described in standard DH-parameters can be found in Table 1. Nonetheless, the method is transferable to other kinematics.

Fig. 1 The energy model of an industrial robot with all comprised losses (variables get introduced in chapter 2).

i	d_i	a_i	α_i	θ_i	offset
1	640 mm	250 mm	$-\pi/2$	q_1	0
2	0	630 mm		q_2	$-\pi/2$
3	0	196 mm	$-\pi/2$	q_3	0
4	807.5 mm	0	$+\pi/2$	q_4	0
5	0	0	$-\pi/2$	q_5	0
6	100 mm	0		q_6	π

Table 1 DH-Parameters of the modeled serial robot Cloos QRC350

The detailed description of the utilized validated energy model of the servo drive system as well as the dynamic model of the mechanical components can be found in [6]. The energy model has been identified and validated in [10]. To adapt the model to the Cloos robot, the parameters for viscous damping, Coulomb friction, and additional motor inertia have been determined using standard identification methods for the warmed up robotic system. The model comprises the following attributes:

- robot dynamics (including mechanical joint couplings),
- gear and motor inertia,
- mechanical power P_{mec},
- DC-bus coupling and multi-axis energy exchange P_{exc},
- friction losses $P_{\mathrm{l,mec}}$,
- operating point-dependent motor and inverter losses $P_{\mathrm{l,M}}$ and $P_{\mathrm{l,I}}$,
- limited DC-bus capacitances and DC-bus losses $P_{\mathrm{l,DC}}$,
- brake resistor dissipation of residual brake energy $P_{\mathrm{l,res}}$,
- supplier losses $P_{\mathrm{l,S}}$,
- auxiliary power supply losses $P_{\mathrm{l,24V}}$.

The consumptions are summarized to calculate the inverter power P_I as follows:

$$P_\mathrm{I}(t) = P_{\mathrm{mec}}(t) + P_{\ell,\mathrm{M}}(t) + P_{\ell,\mathrm{I}}(t). \qquad (1)$$

The consideration of the DC-bus coupling leads to the following formula for the total supply power P_S:

$$P_\mathrm{S}(t) = \left(\sum_{i=1}^{n} P_{\mathrm{I}_i}(t)\right) + P_{\ell,\mathrm{S}}(t) \\ + P_{\ell,24\mathrm{V}}(t) + P_{\ell,\mathrm{DC}}(t), \qquad (2)$$

where *n* is the number of the robot's axes. Negative supply power needs to be dissipated via the brake resistor, since the considered supply module is not able to recuperate:

$$P_{\mathrm{res}}(t) = \begin{cases} P_\mathrm{S}(t), & \text{for } P_\mathrm{S}(t) < 0, \\ 0, & \text{for } P_\mathrm{S}(t) \geq 0. \end{cases} \qquad (3)$$

The storage capacity of the DC-bus capacitor is neglected according to [12]. The supply

power now needs to be cleared of the dissipated brake resistor power:

$$P_S(t) = \begin{cases} P_S(t), & \text{for } P_S(t) > 0, \\ 0, & \text{for } P_S(t) \leq 0. \end{cases} \quad (4)$$

3 THE OPTIMIZATION PROBLEM

The impact of the robot base position on the energy consumption is examined by utilizing a spot welding application, as shown in Fig. 2. The cube represents the workpiece, a detailed description of the examplary task can be found in Section 4.1. The homogenous transformation matrix ^0T_C from the world coordinate system to the first cube corner remains unchanged for the whole evaluation. This simulates a common setup for a robot cell in an automotive production line, where the vehicle body position is predefined while the robot base pose can be varied (within the boundaries of the constraints, as discussed later in this section).

In order to change the robot base pose, the matrix ^0T_B, that describes the homogenous transformation matrix from the world coordinate system to the robot base, needs to be manipulated. The matrix can be segmented as follows:

$$^0T_B = \begin{pmatrix} ^0R_B \in \mathbb{R}^{3\times3} & \rho \\ 0 \quad 0 \quad 0 & 1 \end{pmatrix}, \quad (5)$$

where ^0R_B describes the rotatory and $\rho = [x_B, y_B, z_B]^T$ the translator transformation to the robot base. In general, the only rotational DOF for a robot platform is the rotation around the z-axis; rotations around the other axes strain the mechanical components and are usually not envisaged. Since the here chosen trajectories do not start or end at the home position (the first corner is both the starting and ending point), the rotation around the z-axis is energetically irrelevant, so that $[x_B, y_B, z_B]$
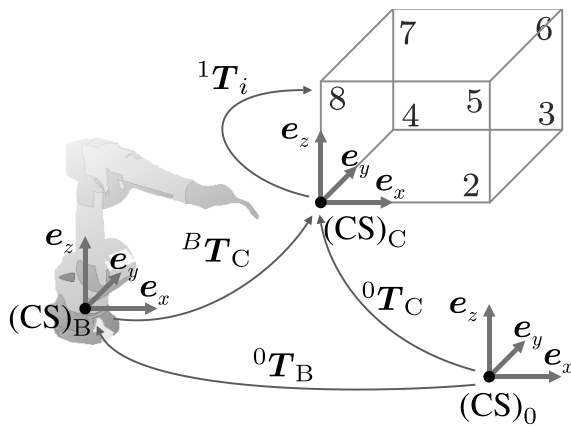
Fig. 2 General configuration of the simulation environment (target corners and base position search space)

remain as the only parameters that need to be optimized. Now, it is necessary to determine the set of joint angles for the respective target corner. The complete homogenous transformation matrix from the robot base pose to a corner *i* can be calculated as follows:

$$^BT_i = \underbrace{(^0T_B)^{-1} \cdot {}^0T_C}_{^BT_C} \cdot {}^1T_i, \quad (6)$$

$$^0T_C = E \in \mathbb{R}^{4\times4}. \quad (7)$$

For every target corner, the joint angle set values $q = [q_1, q_2, ..., q_n]$ can be determined via the inverse kinematic transformation $q = f_{IK}(^BT_i)$. The target orientation for the corners equals the home position orientation (see Table 1). Now, the optimization problem can be formulated as follows:

$$\rho_{opt} = \arg\min_{\rho} J(\rho), \text{subject to:} \quad (8)$$

$$q_{i,\min} \leq q_i(t) \leq q_{i,\max}, \qquad \forall\, i = 1..n, \quad (9)$$
$$|\dot{q}_i(t)| \leq \dot{q}_{i,\max}, \qquad \forall\, i = 1..n, \quad (10)$$
$$|\ddot{q}_i(t)| \leq \ddot{q}_{i,\max}, \qquad \forall\, i = 1..n, \quad (11)$$
$$|\dddot{q}_i(t)| \leq \dddot{q}_{i,\max}, \qquad \forall\, i = 1..n, \quad (12)$$
$$|\dot{\varphi}_{M,i}(t)| \leq \dot{\varphi}_{M,i,\max}, \qquad \forall\, i = 1..n, \quad (13)$$
$$|\dot{\tau}_{M,i}(t)| \leq \dot{\tau}_{M,i,\max}, \qquad \forall\, i = 1..n, \quad (14)$$
$$x_{B,\min} \leq x_B \leq x_{B,\max}, \quad (15)$$
$$y_{B,\min} \leq y_B \leq y_{B,\max}, \quad (16)$$
$$z_{B,\min} \leq z_B \leq z_{B,\max}. \quad (17)$$

The cost function J describes the energy demand of the system and, thus, can be determined by integration of the total supply power P_S:

$$J = \int_{t_0}^{t_1} P_S(\rho, t)\mathrm{d}t, \quad (18)$$

where t_0 is the start and t_1 the end time of the trajectory.

4 MODEL-BADES IMPROVEMENT OF THE ROBOT CELL DESIGN

4.1 EXAMPLARY TASK

The cube in Fig. 2 represents the workpiece that needs to be welded. The homogenous transformation ^0T_C from the world coordinate system to the first cube corner remains unchanged for the whole evaluation. The set path consists of a freely chosen sequence of cube corners which are connected via point-to-point (PTP) movements, i.e. each axis moves to its target position without regarding the resulting trajectory path. The cube corners are described in work space coordinates $x_{EE} = [x, y, z, \alpha, \beta, \gamma]^T$. The homogenous transformation matrix ^BT_i contains the work space coordinates:

$$^{\mathrm{B}}\boldsymbol{T}_i = \begin{pmatrix} ^{\mathrm{B}}\boldsymbol{R}_i(\alpha,\beta,\gamma) \in \mathbb{R}^{3\times3} & \begin{matrix} x \\ y \\ z \end{matrix} \\ \begin{matrix} 0 & 0 & 0 \end{matrix} & 1 \end{pmatrix}. \qquad (19)$$

For the (joint space) path planning between two points, classic synchronized double-S-velocity profiles are utilized for each axis [11]. In order to focus on the base position's effect on the energy consumption, the trajectories deliberately have not been optimized according to [6]. The partial trajectories can now be composed to get the resulting examplary path. In this paper, the corner sequence 1-8-3-5-4-6-1 is chosen:

$$\boldsymbol{q}_{\mathrm{res}}(t) = [\boldsymbol{q}_{18}, \boldsymbol{q}_{83}, \ldots, \boldsymbol{q}_{61}], \qquad (20)$$

where $\boldsymbol{q}_{18}$ is the vector containing the joint angle set values to move from corner 1 to corner 8 (the other vectors are defined accordingly). A pause of one second at each corner represents the spotwelding process. Note that the chosen trajectories do not start or end at the home position. This would adversely affect base positions whose home position is far away from the first corner and, thus, distort the actual impact of the robot base position. The cube edge length is set to 0.75 meters and the robot workload to 10 kilograms (representing mounted welding equipment). The parameters have been chosen to match the robot's workspace and workload dimension. The position of the first cube corner is set to $_{(0)}\boldsymbol{r}_{\mathrm{C}} = [1.25\,\mathrm{m}, 1.25\,\mathrm{m}, 1.75\,\mathrm{m}]$. The restrictions for valid base positions can be used to avoid collisions with other objects within the robot cell. In this example, a cube is defined in which the base position may be freely varied. The constraints for the exploratory robot base positions are chosen so that the workpiece is arranged centrally in front of them:

$$0 \leq x_{\mathrm{B}} \leq 1\,\mathrm{m}, \qquad (21)$$
$$0 \leq y_{\mathrm{B}} \leq 3\,\mathrm{m}, \qquad (22)$$
$$0 \leq z_{\mathrm{B}} \leq 3\,\mathrm{m}. \qquad (23)$$

4.2 COMPARISON OF THE MODELING APPROACHES

The vector $\boldsymbol{\rho}$ (see Section 3) gets discretely varied within the constraints shown in (21)-(23) with a stepsize of 10 centimeters. For every base position, the corresponding energy consumption is calculated for both modeling approaches. The results of the evaluation with the energy model presented in [9] are shown in Fig. 3. Each circle represents a base position while its grey level displays the related energy consumption (black is the energy-optimum). The evaluation of $11 \cdot 21 \cdot 31 = 7161$ grid steps

reveals 596 valid base positions. Base positions that lead to inaccessible joint configurations are eliminated. The seemingly unsteady results at $x = 1.25\,\mathrm{m}$ and $x = 1.75\,\mathrm{m}$ derive from near-singular robot configurations that come up when the base position aligns with the cube edges. The energy values are normalized to the minimal found consumption $E_{\mathrm{min,old}} = 6164\,\mathrm{J}$ to make the comparison of the results of the two approaches easier. Table 2 shows the energy consumption according to the original model E_{old} and according to the proposed model E_{new}.

The same evaluation process is now redone with the proposed energy model described in [6]. The results are displayed in Fig. 4. While the results of the two approaches seem visually alike, a numerical evaluation shows that the complex model finds a different position in terms of overall energy consumption, as shown in Table 2. For the utilized exemplary task and trajectory, additional savings of 4.3 % can be attained. The table also shows the significant impact of considering DC-energy exchange E_{exc} in the modeling equations as well as the high model deviation of approx. 20 %. The results are highly dependent on the considered task and trajectory and can be significantly higher for other examples.

The overall consumption and loss distribution for the worst case, the best case according to the original model, and the best case according to the improved model, are displayed in Fig. 5 (note that all energy consumption values are determined using the proposed energy model). The ratio from the worst to the overall best case of $\frac{E_{\mathrm{max}}}{E_{\mathrm{min}}} = \frac{10\,596\,\mathrm{J}}{7\,433\,\mathrm{J}} \approx 1.43$ confirms the distinct impact of the cell design on the energy consumption. The results also show that even slight misalignment of the base position leads to a significantly higher consumption, so that even processes with small placement scope have energy saving potential. Comparable results were generated with varying parameters, e.g. different target corners, larger or smaller cubes, or a differing workload, always revealing favorable cell designs.

Optimum	E_{old}	E_{new}	E_{exc}
original	6164 J	7768 J	417 J
proposed	6255 J	7433 J	581 J

Table 2 Comparison of the found optimums
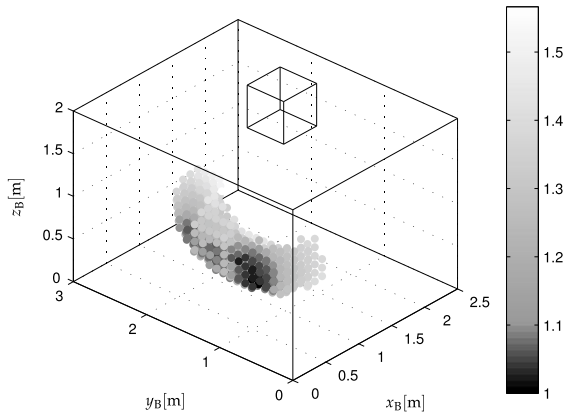
Fig. 3 Energy consumption depending on the robot base position, calculated with the original energy model.
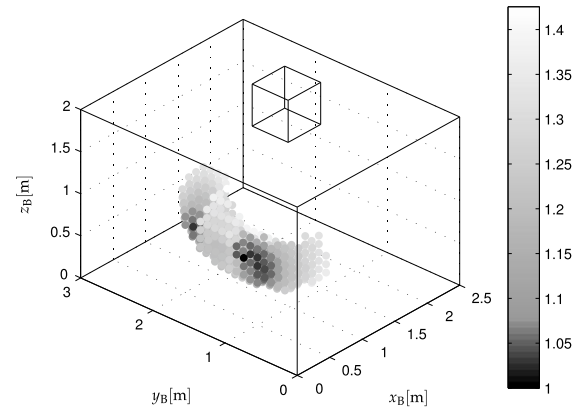
Fig. 4 Energy consumption depending on the robot base position, calculated with the proposed energy model.

5 CONCLUSION

An improved approach to find the energy-optimal position for a robot inside a robot cell has been proposed. In order to show the impact of the robot placement on the energy consumption, a robot including its kinematics, dynamics, path planning, energy demands, and an exemplary task have been modeled. Discrete variations of the base position showed that the energy consumption of a robot is highly dependent on the position of the robot base platform. The comparison of the classical and the proposed energy model shows that the utilization of a complete model that considers every component's losses as well as the DC-bus coupling of the drives is inevitable and leads to better optimization results and, thus, further energy saving potential. The here considered example trajectory allows further 4.3 % saving potential related to the original approach in [9]. Future works will combine the presented method with other efficiency increasing approaches, e.g. simultaneously optimizing the PTP profiles as explained in [6]. The degrees of freedom of the robot base position can be interpreted as additional redundant axes. This could motivate studies for further energy saving potential by using redundant robots (e.g. 6-DOF industrial robots with an additional linear axis or robots with an additional rotary joint).
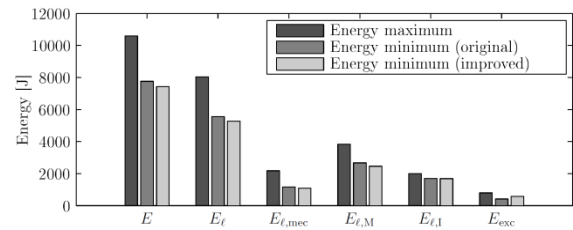
Fig. 5 Loss distribution and energy exchange for the energy-optimum according to the classical and to the proposed approach. The shown consumptions are determined using the proposed energy model.

6 REFERENCES

[1] VDE-Studie Effizienz- und Einspar-potentiale elektrischer Energie, 2008.

[2] Albers, A.; Ottnad, J.; Weiler, H.; Haeussler, P.: "Methods for lightweight design of mechanical components in humanoid robots", in 2007 7th IEEE-RAS International Conference on Humanoid Robots, pp. 609-615, 2007.

[3] Akbaba, M.: "Energy conservation by using energy efficient electric motors", in Applied Energy, Vol. 64, pp. 149-158, 1999.

[4] Meike, D.; Ribickis, L.: "Recuperated energy savings potential and approaches in industrial robotics", in 2011 IEEE International Conference on Automation Science and Engineering, pp. 299-303, 2011.

[5] Pellicciari, M.; Berselli, G.; Leali, F.; Vergnago, A.: "A minimal touch approach for optimizing energy efficiency in pick-and-place manipulators", in The 15th International Conference on Advanced Robotics, pp.100-105, 2011.

[6] Hansen, C.; Oeltjen, J.; Meike, D.; Ortmaier, T.: "Enhanced approach for energy-efficient trajectory generation of industrial robots", in 2012 IEEE International Conference on Automation Science and Engineering, 2012.

[7] Hsu, D.; Latombe, J.-C.; Sorkin, S.: "Placing a robot manipulator amid obstacles for optimized execution", in Proceedings of the 1999 IEEE International Symposium on Assembly and Task Planning, pp. 280-285, 1999.

[8] Vosniakos, G.-C.; Matsas, E.: "Improving feasibility of robotic milling through robot placement optimization", in Robotics and Computer-Integrated Manufacturing, pp. 517-525, 2008.

[9] Ur-Rehman, R.; Caro, S.; Chablat, D.; Wenger, P.: "Path placement optimization of manipulators based on energy consumption: application to the Orthoglide 3-axis", in Transactions of the Canadian Society for Mechanical Engineering, Vol. 33, No. 3, pp. 523-541, 2009.

[10] Hansen, C.; Kotlarski, J.; Ortmaier, T.: "Experimental validation of advanced minimum energy robot trajectory optimization", in 2013 16th International Conference on Advanced Robotics, 2013.

[11] Biagiotti, L.; Melchiorri, C.: Trajectory planning for automatic machines and robots, Springer Verlag, 2008.

[12] dos Santos, R. R.; Steffen Jr., V.; Saramago, S. F. P.: "Robot path planning in a constrained workspace by using optimal control techniques", in Multibody System Dynamics, Vol. 19, pp. 159-177, 2008.

_____

Author:	Eggers, Kai; Hansen, Christian; Kotlarski, Jens; Ortmaier, Tobias
University:	Leibniz Universität Hannover
Department:	Institut für Mechatronische Systeme
E-Mail:	{kai.eggers, christian.hansen, jens.kotlarski, tobias.ortmaier}@ imes.uni-hannover.de

_____